Time-resolved phase-sensitive second harmonic generation spectroscopy

Paweł J. Nowakowski, David A. Woods, Colin D. Bain, and Jan R. R. Verlet

Citation: The Journal of Chemical Physics **142**, 084201 (2015); doi: 10.1063/1.4909522
View online: http://dx.doi.org/10.1063/1.4909522
View Table of Contents: http://scitation.aip.org/content/aip/journal/jcp/142/8?ver=pdfcov
Published by the AIP Publishing

Articles you may be interested in

Femtosecond time-resolved photoelectron spectroscopy with a vacuum-ultraviolet photon source based on laser high-order harmonic generation
Rev. Sci. Instrum. **82**, 063114 (2011); 10.1063/1.3600901

Influence of the photodepoling parameters on quasiphase-matched second-harmonic generation and optical parametric fluorescence in polymer channel waveguides
J. Appl. Phys. **96**, 7112 (2004); 10.1063/1.1809770

Second-harmonic generation and Maxwell displacement current spectroscopy of chiral organic monolayers at the air–water interface
J. Chem. Phys. **119**, 7427 (2003); 10.1063/1.1605943

Photoinduced phase-matched second-harmonic generation in azodye-doped polymer films
J. Appl. Phys. **89**, 2029 (2001); 10.1063/1.1343890

Optical control of third-harmonic generation in azo-doped polymethylmethacrylate thin films
Appl. Phys. Lett. **77**, 2095 (2000); 10.1063/1.1314878

This article is copyrighted as indicated in the article. Reuse of AIP content is subject to the terms at: http://scitation.aip.org/termsconditions. Downloaded to IP: 129.234.252.66 On: Thu, 26 Mar 2015 14:17:19

Time-resolved phase-sensitive second harmonic generation spectroscopy

Paweł J. Nowakowski, David A. Woods, Colin D. Bain, and Jan R. R. Verlet[a)]
Department of Chemistry, Durham University, Durham, DH1 3LE, United Kingdom

(Received 19 December 2014; accepted 6 February 2015; published online 23 February 2015)

A methodology based on time-resolved, phase-sensitive second harmonic generation (SHG) for probing the excited state dynamics of species at interfaces is presented. It is based on an interference measurement between the SHG from the sample and a local oscillator generated at a reference together with a lock-in measurement to remove the large constant offset from the interference. The technique is characterized by measuring the phase and excited state dynamics of the dye malachite green at the water/air interface. The key attributes of the technique are that the observed signal is directly proportional to sample concentration, in contrast to the quadratic dependence from non-phase sensitive SHG, and that the real and imaginary parts of the 2nd order non-linear susceptibility can be determined independently. We show that the method is highly sensitive and can provide high quality excited state dynamics in short data acquisition times. © *2015 AIP Publishing LLC*. [http://dx.doi.org/10.1063/1.4909522]

I. INTRODUCTION

Many chemical, physical, and technological processes occur at the interface between two media and these can significantly differ from the analogous process in either media, or indeed entirely new mechanisms can emerge that have no bulk analogue. Hence, the study of interfacial dynamics has attracted a broad interest in diverse fields including biochemistry, atmospheric and astrochemistry, electrochemistry, and analytical chemistry. The experimental study of interfaces has been greatly aided by the development of even-order nonlinear spectroscopy. Phenomena such as second harmonic generation (SHG) or sum frequency generation (SFG) can only occur in non-centrosymmetric media because of symmetry restrictions within the electric dipole approximation. In a medium with inversion symmetry, even-order processes are forbidden, while at the interface between two such media, this symmetry is necessarily broken. As a result, even-order nonlinear spectroscopy can be surface specific to less than a monolayer. To gain species selectivity, resonance-enhancement can be used, where either of the driving fields or the second-order nonlinear field produced is in resonance with a transition of the species of interest at the interface. This also serves to enhance the SHG or SFG signals relative to the inherent non-linear signal generated from the interface, thus enabling the study of the spectroscopy and dynamics of adsorbates at interfaces. SHG and SFG are described in detail in a number of standard textbooks,[1,2] and the study of adsorbates at interfaces using SHG and SFG has been the focus of a number of excellent reviews.[3–7]

Unfortunately, the non-linear signal is often very weak and this is a particular problem when the interfacial concentration of the adsorbate species is small. This situation generally arises for time-resolved measurements in which a pump pulse only excites a small fraction of adsorbates to induce the process of interest that is subsequently probed by SHG or SFG. The resulting resonance-enhanced signal can then be difficult to distinguish from the nascent interface background and can interfere with it.[8] Here, we describe a method for probing the ultrafast dynamics at interfaces using SHG in which the interference with a local oscillator (LO) is used to enhance sensitivity, to linearize the measured SHG signal with respect to interfacial concentration, and to enable phase-sensitive measurements.

The polarization, $\mathbf{P}$, induced in a material by the electric field of light, $\mathbf{E}$, can be expressed as a power series,

$$\mathbf{P} = \mathbf{P}_0 + \chi^{(1)}\mathbf{E} + \chi^{(2)}\mathbf{E}\cdot\mathbf{E} + \cdots, \tag{1}$$

where $\chi^{(1)}$ is the linear and $\chi^{(n)}$ the nth-order non-linear susceptibility. When the driving field is weak, only the term linear in $\mathbf{E}$ is important (the static polarization, $\mathbf{P}_0$, can usually be neglected because it does not radiate); however, at higher field strengths the second- (and higher-) order terms become significant. For SHG, both driving fields are at the same frequency, and the second-order term leads to an emitted field at twice the input frequency. All molecular information is contained in the second order susceptibility, $\chi^{(2)}$, which can be written as

$$\chi^{(2)} = N_S \langle\beta\rangle, \tag{2}$$

where N_S is the number of adsorbates per unit area and $\langle\beta\rangle$ is the orientationally averaged hyperpolarizability of the species. However, when monitoring a specific adsorbate through resonance-enhancement, two terms contribute to the effective second-order susceptibility

$$\chi^{(2)}_{\text{eff}} = \chi^{(2)}_{\text{R}} + \chi^{(2)}_{\text{NR}}, \tag{3}$$

where $\chi^{(2)}_{\text{R}}$ contains resonant contributions (and is proportional to N_S) and $\chi^{(2)}_{\text{NR}}$ all other non-resonant contributions arising from the nascent interface. Note that $\chi^{(2)}$ in general is a complex quantity. If the probe is on resonance with the adsorbate, then $\chi^{(2)}_{\text{R}}$ is predominantly imaginary. In contrast, $\chi^{(2)}_{\text{NR}}$ is real (if sufficiently far from resonance). The signal measured in a SHG

a)Author to whom correspondence should be addressed. Electronic mail: j.r.r.verlet@durham.ac.uk

 © 2015 AIP Publishing LLC

This article is copyrighted as indicated in the article. Reuse of AIP content is subject to the terms at: http://scitation.aip.org/termsconditions. Downloaded to IP: 129.234.252.66 On: Thu, 26 Mar 2015 14:17:19

experiment, S_{SHG}, is the square of the generated SHG electric field

$$S_{SHG} = \mathbf{E}_{SHG}^2 \propto \left|\chi_R^{(2)} + \chi_{NR}^{(2)}\right|^2 I^2 = \left[\left|\chi_R^{(2)}\right|^2 + \left|\chi_{NR}^{(2)}\right|^2 + 2\left|\chi_R^{(2)}\right|\left|\chi_{NR}^{(2)}\right|\cos\varphi\right] I^2. \quad (4)$$

The interference term between $\chi_R^{(2)}$ and $\chi_{NR}^{(2)}$ means that, when measuring resonance-enhanced S_{SHG} of an adsorbate (which is contained in $\chi_R^{(2)}$), the signal can depend on N_S to any power between 1 and 2. In the limit that $\chi_R^{(2)} \gg \chi_{NR}^{(2)}$, $S_{SHG} \propto N_S^2$, while in the limit that $\chi_R^{(2)} \ll \chi_{NR}^{(2)}$, $S_{SHG} \propto N_S$. Consequently, a direct comparison with linear bulk spectroscopic measurements such as transient absorption becomes difficult. An elegant way to overcome the above difficulties is by using interference, which can provide a signal linear in concentration, and information about the phase can help to distinguish the imaginary part, corresponding to the resonant part, from the background.

The importance of measuring the phase of the nonlinear susceptibility has been demonstrated as early as 1965, when Chang *et al.*[9] reported the first phase sensitive measurement of SHG. In this, the second harmonic generated by reflection from a surface was interfered with a second SHG beam (later called the local oscillator, $\mathbf{E}_{LO}$) generated from a second surface but from the same fundamental beam. The phase-delay between the two wavelengths of light was controlled by varying the pressure of air between the two surfaces.

Recently, the range of different approaches to phase-sensitive SHG and SFG has been reviewed;[10] we briefly discuss the main methods below. Interference measurements of SHG were exploited extensively in the 1980s for studying adsorbates at interfaces.[11–13] Phase-sensitive measurements were also applied to SFG[14–18] and sum-frequency vibrational spectroscopy (SFVS), which have attracted a considerable attention because of its ability to probe vibrational spectra of the molecules at interfaces. Phase-sensitive SFVS measurements can also provide information about the absolute orientation of specific functional groups in the adsorbate. A limitation of early phase-sensitive measurements was that, to obtain a vibrational spectrum, the IR probe beam had to be scanned over the spectral region of interest, making the measurements time consuming. More recently, this has been overcome by the use of broadband lasers and the collection of the entire spectrum using heterodyne-detected (HD) SHG[19,20] and SFG spectroscopy.[21–30] In this, the signal and local oscillator are separated in time at a fixed delay and the interference is essentially measured in the frequency domain. By back-Fourier transformation, filtering and forward-Fourier transformation, the real and imaginary parts of the non-linear susceptibility can be measured across a spectral range. These types of measurements have also been extended to the time-domain in which the spectral evolution is monitored as a function of time.[29,31,32] Although such experiments are extremely insightful, they are also very time-consuming and consequently require phase-stability over several hours, which can be non-trivial. As a result, such experiments may become prohibitively difficult for measuring the ultrafast dynamics of species at low concentration. To overcome this, we have developed a method that uses an interference-measurement and monitors the integral time-resolved SHG signal. Although the differential nature of HD-SHG has been lost, our method is superior in terms of sensitivity and phase-stability. The distance between sample and reference only requires mm precision.

II. METHODOLOGY

The basic idea of the phase-sensitive measurement follows one of the methods reviewed by Stolle *et al.*,[33] where the second harmonic is generated from the sample in reflection, $\mathbf{E}_{SHG}$, and travels collinearly with the remaining reflected fundamental onto a reference surface. At the reference surface, the remaining reflected fundamental light produces the local oscillator SHG field, $\mathbf{E}_{LO}$, that will interfere with $\mathbf{E}_{SHG}$. Spatial overlap is guaranteed by the fact that the beam paths are identical. The measured interference signal can be expressed as

$$S^i = |\mathbf{E}_{SHG}|^2 + |\mathbf{E}_{LO}|^2 + 2f(L)\,|\mathbf{E}_{SHG}|\,|\mathbf{E}_{LO}|\cos\left(\varphi + \frac{2\pi\omega\Delta n}{c}L\right), \quad (5)$$

where φ is the phase between $\mathbf{E}_{SHG}$ and $\mathbf{E}_{LO}$ at the point they are generated and ω is the angular frequency of the second harmonic light. The phase can be controlled by virtue of the differing phase velocities of the driving field and the SHG fields in air (due to the difference in refractive index, Δn, at the two wavelengths) and, hence, can be conveniently controlled by altering the distance between the sample and the reference surfaces, L. If this distance is relatively small, then the group velocity mismatch is sufficiently small that both pulses remain temporally overlapped. Nevertheless, some attenuation will occur because of the group-velocity mismatch, which is included in Eq. (5) through the function $f(L)$. The term of interest is the interference term in Eq. (5) as this is linear in $\mathbf{E}_{SHG}$ and therefore in also concentration. To measure this term without the (large) constant offset imposed by the $\mathbf{E}_{SHG}{}^2$ and $\mathbf{E}_{LO}{}^2$ terms, one can employ a lock-in measurement.

The lock-in measurement consists of two separate measurements. The first one occurs as described above, where $\mathbf{E}_{SHG}$ and $\mathbf{E}_{LO}$ temporally overlap. In a second measurement, the fundamental and $\mathbf{E}_{SHG}$ beams are passed through a dispersive material which is placed between the sample and the reference surfaces. The result is that the group velocity mismatch between the harmonic and second harmonic is sufficiently large such that the two short pulses no longer temporally overlap. Hence, $\mathbf{E}_{LO}$ will be generated before the $\mathbf{E}_{SHG}$ pulse arrives at the reference surface and they can therefore not interfere. As a result, from the second measurement, $S^i = |\mathbf{E}_{SHG}|^2 + |\mathbf{E}_{LO}|^2$. The difference between the two measurements yields the interference term of interest,

$$S^{lock-in} = 2f(L)\,|\mathbf{E}_{SHG}|\,|\mathbf{E}_{LO}|\cos\left(\varphi + \frac{2\pi\omega\Delta n}{c}L\right). \quad (6)$$

A simple scheme of the measurement is shown in Figure 1. The method works because of the integration over the entire pulse envelope in the frequency domain. If we attempted to record the spectrum by dispersing it onto a spectrometer, then the measurement yielding $S^i = |\mathbf{E}_{SHG}|^2 + |\mathbf{E}_{LO}|^2$ would be

This article is copyrighted as indicated in the article. Reuse of AIP content is subject to the terms at: http://scitation.aip.org/termsconditions. Downloaded to IP: 129.234.252.66 On: Thu, 26 Mar 2015 14:17:19

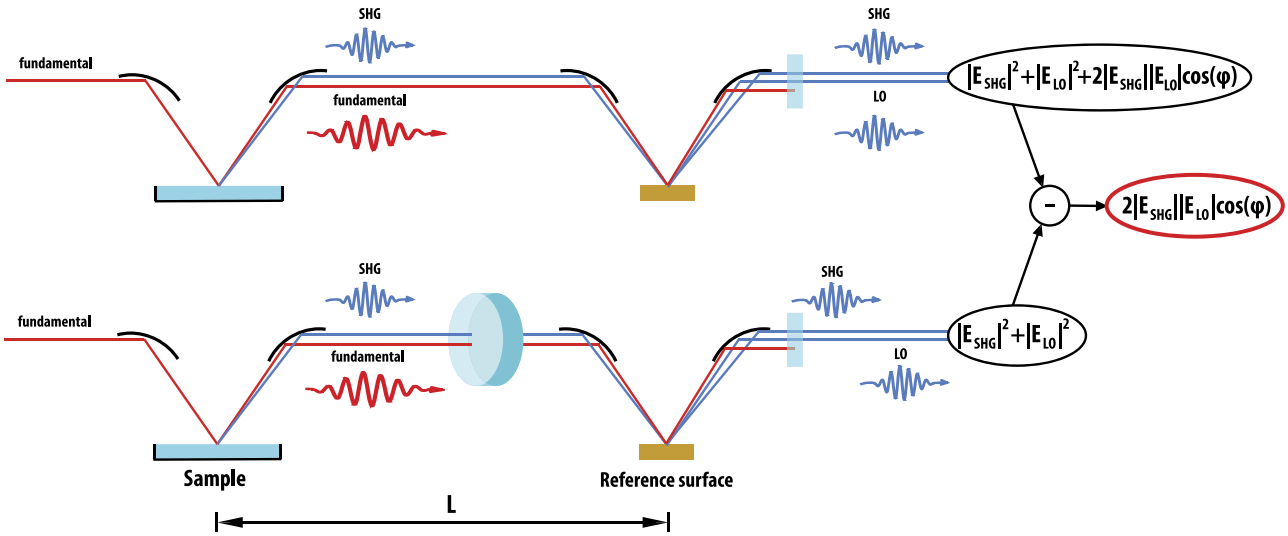

FIG. 1. Schematic representation of the lock-in measurement. The top path shows the interference of a SHG field generated from the surface of interest with a LO from a reference surface. The bottom path shows the same, but the SHG and fundamental that will generate the LO are offset in time by the presence of a dispersive material leading to a group-velocity mismatch. In such a case, no interference takes place. The difference between the measurements recovers the interference term of interest.

similar to the heterodyne detected methods, and would show an interference pattern superimposed onto the spectral envelope, which depends on the temporal delay between the two pulses.

III. EXPERIMENTAL

A schematic of the experimental setup is shown in Figure 2. Our main scientific interests are in ions at aqueous interfaces, and to demonstrate the methodology, we study the ambient water/air interface with malachite green (MG) as a cationic adsorbate. All laser pulses were derived from a commercial femtosecond laser system based on a Ti:Sapphire oscillator and a chirped pulse amplifier (Tsunami and Spitfire Pro XP, Spectra-Physics), providing 35 fs pulses with a 3 mJ pulse energy centered around 800 nm. The system was operated at 333 Hz.

For the probe beam, either attenuated 800 nm light from the amplifier was used directly, or the signal output from a commercial optical parametric amplifier (TOPAS Prime, Spectra-Physics) at 1220 nm was used. The pump was generated by SHG of the fundamental in a BBO crystal, providing 400 nm light. Both the pump and the probe pulses were linearly polarized in the plane of reflection (*p* polarized). The beams were independently focused by a pair of curved mirrors onto sample surface at a ~70° angle of incidence. In order to refresh the sample, it was placed in a dish that was rotated with an angular velocity of ~0.7 rad/s. The delay between pump and probe pulses was controlled by a home-built mechanical delay

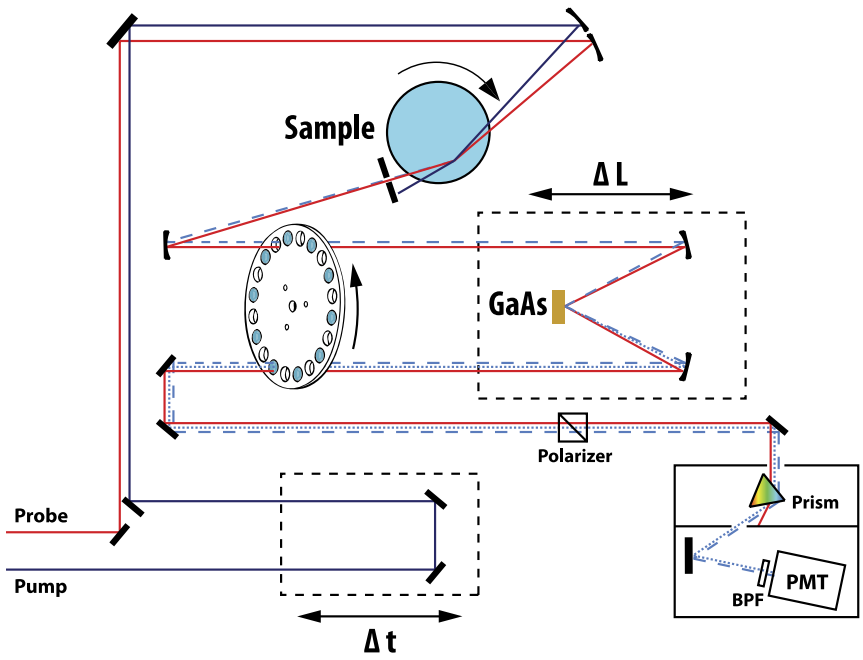

FIG. 2. Schematic of the experimental setup. The red line indicates a path of the probe beam, the dark blue solid line is a path of the pump beam, and the light blue is a path of a second harmonic from the sample (dashed line) and local oscillator (dotted line). BPF is a band pass filter and PMT is a photomultiplier tube. The dashed rectangles indicate positions of the translation stages, with arrows showing the direction of motion.

This article is copyrighted as indicated in the article. Reuse of AIP content is subject to the terms at: http://scitation.aip.org/termsconditions. Downloaded to IP: 129.234.252.66 On: Thu, 26 Mar 2015 14:17:19

stage, capable of changing the delay in steps as small as ~3 fs. After the sample, any reflected pump beam was blocked. The reflected collinearly propagating probe and its SHG from the sample were then collimated using a curved metal mirror and entered the interference setup.

As a reference surface (110)-cut gallium arsenide (GaAs) was used. To change the distance, L, between the sample and the reference surface, a manual translation stage was used, on which the reference surface and two focusing mirrors were placed as shown in Figure 2. In order to generate a lock-in measurement on a shot-to-shot basis, a rotating chopper was placed between the sample and the reference. The custom chopper wheel consisted of 20 holes, where in every second hole, an SF10 glass window (2 mm thickness) was placed in order to provide the aforementioned group velocity difference between the SHG from the sample and the fundamental pulses.

After the generation of the LO, both the SHG and LO beams were directed on a pair of mirrors and directed through the chopper once more. This was done to compensate for losses introduced by reflections from the SF10 windows. The setup was aligned in such a way that for every shot, the beams pass through the SF10 window once (i.e., if the SF10 window is present between the sample and LO, it is *not* present after the LO, and vice versa). This arrangement ensured that the SHG from the sample always passes through an SF10 window, which in turn ensured that the $|\mathbf{E}_{\mathrm{SHG}}|^2$ term from Eq. (5) (which could vary with experimental conditions) was cancelled in the final lock-in measurement. However, a small constant offset remained, due to a difference in the reflection losses depending on whether the LO beam passes through the window or the fundamental beam that generates the LO passes through the glass window. A detailed consideration of this offset is given in the supplementary material.[34] For SF10 windows with a 800 or 1220 nm probe beam, the offset is approximately $+0.15|\mathbf{E}_{\mathrm{LO}}|^2$ or $+0.1|\mathbf{E}_{\mathrm{LO}}|^2$, respectively. We have not removed this offset from measurements of signal with as a function of the stage position (e.g., Figure 3, later). However, we have removed the offset from our pump-probe measurements, where the signal should be proportional to concentration. A possible minor source of errors in our subtraction occurs because the reflectance of the fundamental from the sample is a function of the state of the sample. In practice signals from a dye solution

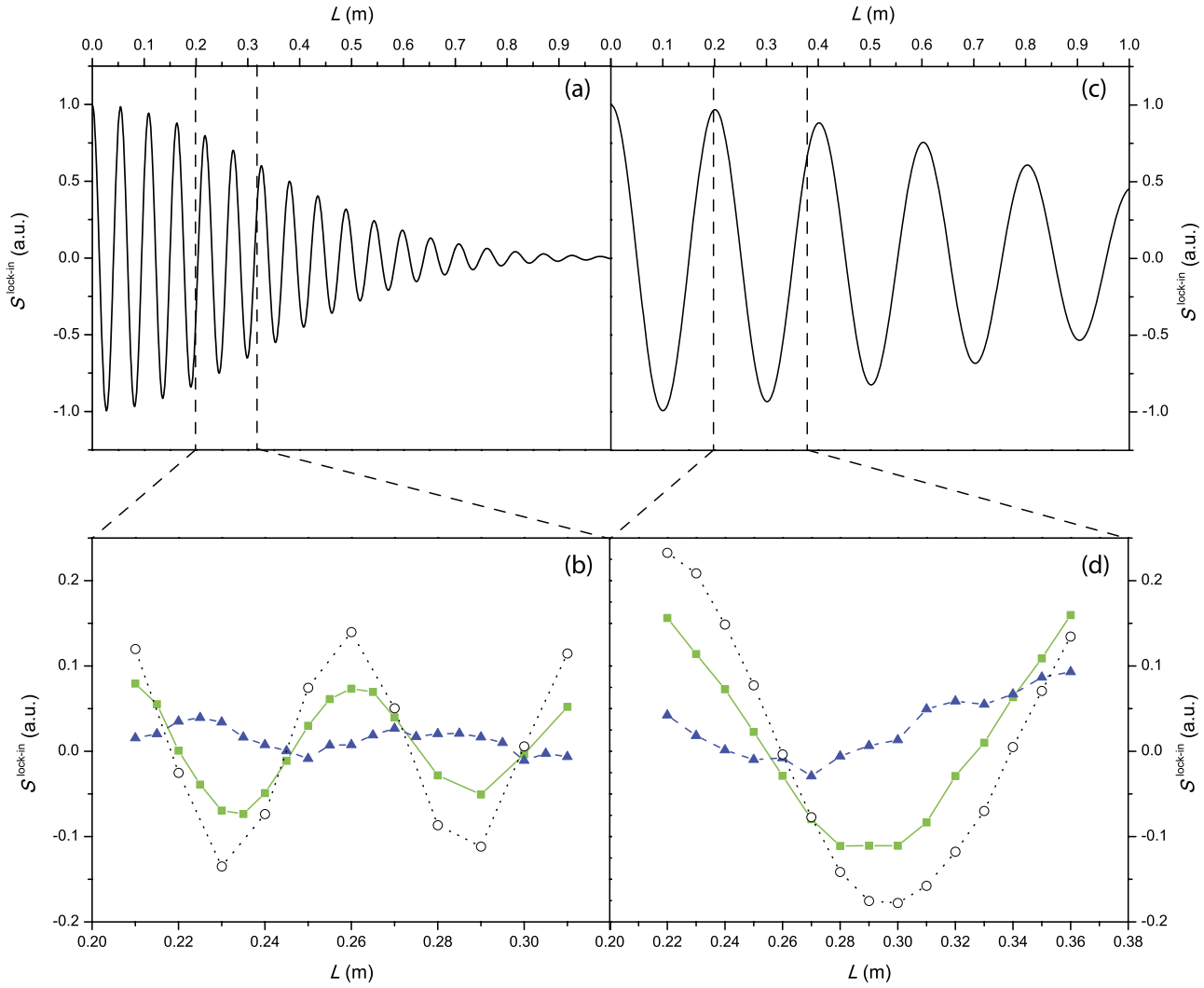

FIG. 3. Dependence of interference signal on distance between sample and reference surface L. (a) Calculated signal and (b) measured signal with a 800 nm probe beam; (c) calculated signal; and (d) measured signal for a 1220 nm probe beam. The green squares represent signal obtained with malachite green as a sample, blue triangles represent water signal (10× for (b) and 5× for (d)) and open circles represent quartz.

This article is copyrighted as indicated in the article. Reuse of AIP content is subject to the terms at: http://scitation.aip.org/termsconditions. Downloaded to IP: 129.234.252.66 On: Thu, 26 Mar 2015 14:17:19

and water are unlikely to be directly comparable, while signals from a dye solution before and after photo-bleaching should be comparable.

The beams were then directed through a Glan-Taylor polarizer, where a specific polarization was selected (p-polarized). Finally, the beams entered a light-tight box in which the fundamental beam was separated from the SH and LO beams using a prism, and the interference between SH and the LO beams was detected by a photomultiplier tube (PMT) (Hamamatsu H7732-10).

The output from the PMT was recorded across a 250 kΩ resistor using a DAQ card (NI-USB-6210) and monitored over ~1000 laser shots. Each pulse was integrated and divided into odd (A) and even (B) pulses, corresponding to the full form and only quadratic terms of Eq. (5), respectively. The lock-in interference signal was then simply calculated as $S^{\text{lock-in}} = A - B$, and averaged over all shots.

To quantify and calibrate the absolute phase, a piece of left-handed z-cut quartz was used in the place of the sample, and placed so that the positive x-axis was oriented along the direction of beam propagation in the plane of incidence. The positive x-axis was defined using the piezo-electric effect[35] and determined by measuring the sign of the brief potential generated when the quartz was squeezed in its xy-plane using a clamp. Because of a lack of absorption in the wavelength range used, the signal obtained from quartz contains only the nonresonant (real) part in Eq. (4).[36] However, as quartz is a bulk-SHG active material an additional factor of i, and thus a phase difference of $\pi/2$, should be added.[37] Therefore, we would expect quartz to have a similar phase to that of a resonant adsorbed layer.

IV. RESULTS AND DISCUSSION

As a proof-of-concept, we have studied the excited state dynamics of MG at the water/air interface. MG has been the subject of a number of investigations before, including at the water/air interface using time-resolved SHG, and it therefore serves as an ideal comparator. Additionally, it has optical transitions ($S_1 \leftarrow S_0$ and $S_2 \leftarrow S_0$ at 610 and 400 nm, respectively) that are readily accessible for resonant enhancement and provides a strong SHG (and SFG) signal.[38,39] All reported experiments used a 10 μM solution of MG in water.

To determine the relative phase of the measurements and the phase-stability, the lock-in signal was measured as a function of the distance L (see Figure 2); $S^{\text{lock-in}}(L)$. Note that no pump beam was present for these measurements. The results are shown in Figure 3 for both an 800 nm and 1220 nm probe beam. Also shown in Figure 3 is the expected signal based on the relative phase-velocities in air between 800 and 400 nm and 1220 and 610 nm (assuming ~30 fs FWHM Gaussian transform-limited pulses—full details of the calculations are given in the supplementary material[34]). The oscillations arise from the SHG and LO being in phase (constructive interference) or out of phase (destructive interference), while the envelope arises from the group-velocity mismatch. The oscillation frequency and damping are faster for the 800 and 400 nm case because of the more rapidly changing nature of the refractive index of air between those two wavelengths than at 1220 and 610 nm.

The measured response over the range $0.2 < L < 0.4$ m reproduces the calculated interference pattern. Also included in Figure 3 are the results for an experiment in which quartz was used as a sample. Comparing the signal detected from MG with the signal from quartz shows that these are almost in phase. As mentioned before, this suggests that the signal from MG at the probed wavelengths mostly contains the imaginary part of $\chi^{(2)}_{\text{R}}$. This is in line with the fact that 610 nm is resonant with the $S_1 \leftarrow S_0$ transition, while 400 nm is resonant with the $S_2 \leftarrow S_0$ transition. Removing all MG leaves only the water/air interface, and the probe wavelengths are far from any water resonances. In such a case, the signal should be dominated by $\chi^{(2)}_{\text{NR}}$ which is mostly real and we would expect to see a $\pi/2$ phase difference. This is indeed what is observed in Figure 3 for the water/air interface relative to the MG solution. Note that the signal from water is also much weaker than that from MG. Errors can be obtained experimentally from the statistics of multiple shots at the same stage position. However, the main source of error is due to slow drifts in the optical alignment either due to sample evaporation or imperfect alignment of the optical delay line. This is most apparent for very low signal levels as is the case for pure water (see Figure 3).

Figure 3 demonstrates that the experiment is phase-stable to relative displacements between the SHG and LO on the order of centimeters. Because all beams are in fact collinear at all times, any phase instability arises from changes in the refractive index of air. Hence, the experiment is essentially phase-stable. The decrease of interference arising from the group-velocity mismatch becomes greater for shorter wavelengths. At present, the minimum distance between sample and reference surfaces is 0.20 m, which means that we are in practice limited to probe wavelengths $\lambda > 600$ nm for 40 fs pulses. Shorter useable probe wavelengths can be attained by either using longer pulses or by miniaturization of the set-up.

It is worth briefly considering how the signal to noise (S/N) can be maximized in the experiment. If the main source of noise is due to the Poisson distributed shot-noise, then the signal is linearly proportional to $|\mathbf{E}_{\text{LO}}|$, while the noise becomes linear with the electric field at the local oscillator around the point that $|\mathbf{E}_{\text{LO}}| > |\mathbf{E}_{\text{SHG}}|$. Therefore, to maximize S/N, the contribution from the local oscillator should be significantly greater than that from the sample. Once this limit is reached, however, there is no benefit from further increasing the LO strength (an increase in signal gives an equivalent increase in noise).[28] Of course, a major benefit is that the reference surface can be chosen such that $\mathbf{E}_{\text{LO}}$ is large and therefore the detection limit is not limited by the detector as is the case in conventional SHG spectroscopy. There is a small S/N advantage in conducting the experiment in destructive rather than constructive inference, since the difference signal remains the same, but one of the two individual signals is smaller and thus has less noise. Under these conditions, there is actually an optimal point above which increasing the LO strength (slightly) decreases S/N. Other sources of noise can directly affect the lock-in measurement and care should be taken to avoid them: we perform our experiment at 333 Hz to avoid picking up mains noise at overtones of 50 Hz; reflected ambient light from the

This article is copyrighted as indicated in the article. Reuse of AIP content is subject to the terms at: http://scitation.aip.org/termsconditions. Downloaded to IP: 129.234.252.66 On: Thu, 26 Mar 2015 14:17:19

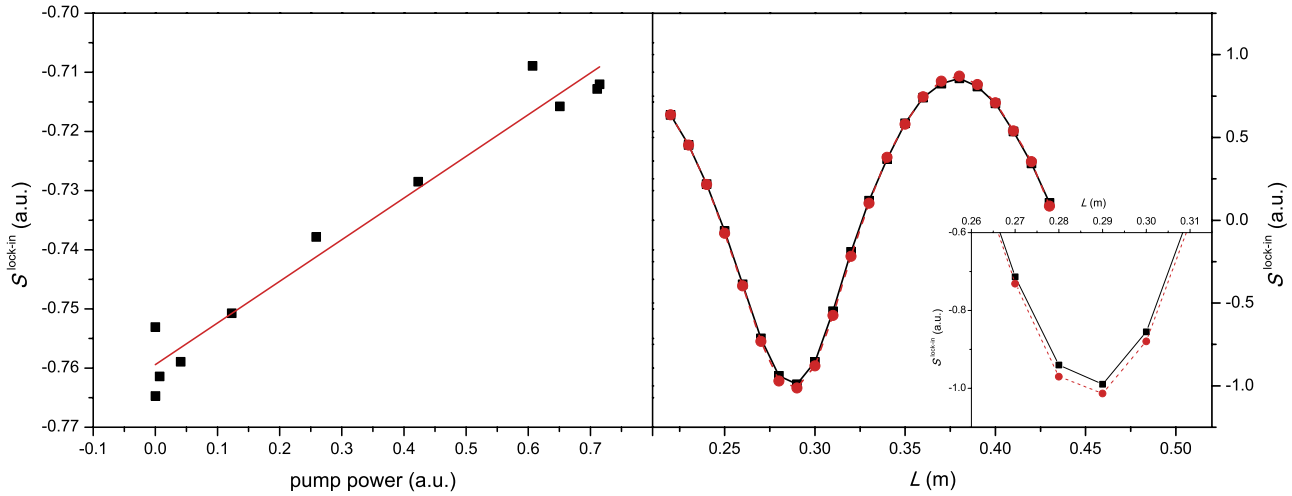

FIG. 4. Left: Interference signal obtained with the varied pump power, taken at the distance between the surfaces $L = 0.29$ m, with the red line indicating linear fit. Right: The interference signal, with varying distance L, in absence of pump beam (red circles) and with a pump beam at maximum power (black squares), with a magnification of the destructive interference peak in the inset.

chopper windows can appear in the lock-in signal; and white light generated by focusing the probe beam into the sample can also be detected with an intensity that depends on the chopper position.

The linearity of the technique with interfacial concentration can be determined using a pump-probe experiment. Specifically, a pump pulse at 400 nm drives the $S_2 \leftarrow S_0$ transition while a probe at 1220 nm is proportional to the number of MG molecules in S_0. Thus, a well-timed 400 nm pump pulse will remove some of the population from S_0 so that the measured signal from the probe will be depleted. By linearly varying the pump power, the interfacial concentration of MG in S_0 will also be varied linearly. The delay between pump and probe was set to 300 fs, and the subsequent interference signal was measured by varying the pump power by rotating a $\lambda/2$ plate placed before the BBO crystal that produces the 400 nm. The maximum pump energy (~1 μJ pulse^{-1}) was kept sufficiently low to ensure that no saturation effects were introduced as this would lead to a non-linearity of the concentration as a function of pump pulse energy. The results are shown in Figure 4. This shows a linear dependence of the interference signal as a function of interfacial concentration. The right panel of Figure 4 shows the difference in signal as a function of phase when the pump is present and absent.

Figure 4 demonstrates that the interference-based signal is linear with concentration. Hence, a time-resolved pump-probe measurement can now be considered linear. To probe the dynamics of the recovery of the S_0 state following excitation to S_2, MG was excited with a 400 nm pump (23 μJ pulse^{-1}) and probed at variable delays using 1220 nm (50 μJ pulse^{-1}). Figure 5 shows the recovery of photo-excited MG to its S_0 ground state.[38] The distance L between sample and reference surface was set so that the SHG and LO were in destructive interference.

Immediately after excitation, the ground state is bleached as shown by a decrease in signal at zero delay between pump and probe pulses. After ~20 ps, the signal recovers and then decays further on a much longer time-scale. The data points in Figure 5 represent a single measurement where each point is an average of 3300 pulses (10 s). Hence, the entire trace could be measured in <10 min. The solid line in Figure 5 is the average of 10 successive measurements (~1 h), demonstrating the ability in acquiring high quality data in relatively quick time. Comparing our data with that measured by Sen *et al.*[39] using the conventional SHG (proportional to $|\chi^{(2)}|^2$) reveals very similar dynamics and timescales when the square-root of their raw data is considered. In terms of signal to noise, our single run data-set (which contains about twice as many data-points over the first 30 ps) is of comparable quality as that presented by Sen *et al.*[39]

The method presented here does take a shortcut to acquiring data quickly: the lock-in measurement is based on two points (with and without interference) and thus does not distinguish between a decreasing amplitude of the interference pattern (change in surface concentration) and a phase shift with a constant amplitude (change in absorption spectrum). Figure 6 illustrates this graphically. To clarify the ambiguity, either the interference pattern (as in Figures 3 and 4) can be recorded at a few select pump-probe delays, or the dynamics at a number of different phase differences between 0 and π can be measured. For the data presented here on MG, there was only a change in amplitude and no significant phase shift (inset of Figure 5).

Finally, we compare the technique developed here to the two most commonly used methods of measuring phase-sensitive SHG. The standard (non-spectroscopic) technique of measuring an interference curve,[40] similar to those here given in Figure 3, is challenging to do in a time-resolved manner, since it either requires the curve to be repeated at each time-point (which is time consuming) or it becomes very sensitive to small long-term drifts in laser power or alignment, due to the large offset from the quadratic terms in Eq. (5). In contrast, our lock-in measurement makes the time-resolved measurement very quick and comparatively insensitive to drifts in laser power or alignment since we eliminate the vast majority of the offset.

The heterodyne detected technique has the major advantage of recording a spectral profile, which our technique cannot readily do. The bandwidth we integrate over would need to be

This article is copyrighted as indicated in the article. Reuse of AIP content is subject to the terms at: http://scitation.aip.org/termsconditions. Downloaded to IP: 129.234.252.66 On: Thu, 26 Mar 2015 14:17:19

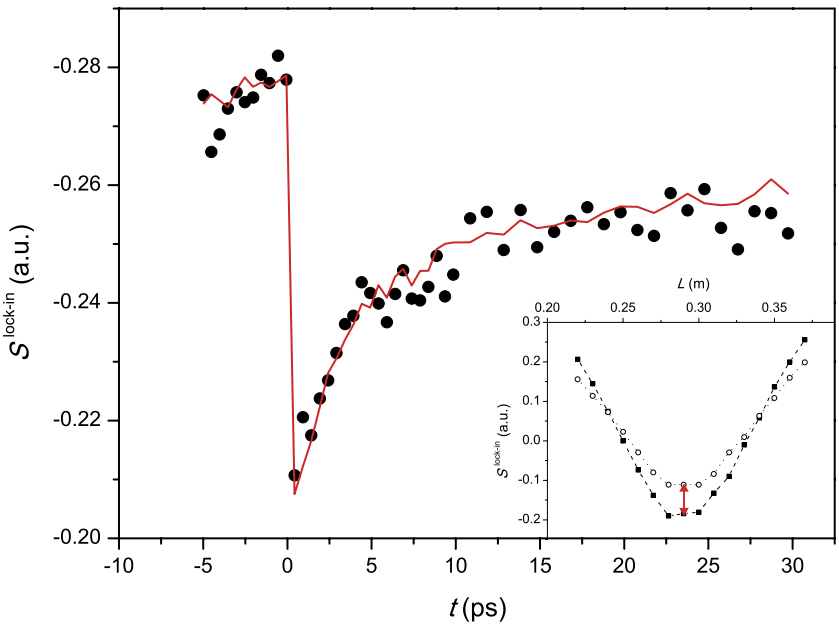

FIG. 5. Time resolved spectra of the recovery of the ground state MG. The red solid line shows an average of 10 measurements, while the dots show a single measurement. The inset presents an interference signal obtained in the presence (empty circles and dotted line) and absence (filled squares and dashed line) of the pump beam with varying distance L, with arrow showing the position at which the time resolved measurement was taken.

large compared to $1/\Delta t$, where Δt is the delay between the sample and local oscillator pulses in the "B" measurement. Although, in principle, a spectroscopic measurement could be achieved (replacing our PMT with a CCD) by using much thicker windows, in practice this is unlikely to be feasible. The group velocity dispersion of the pulses as they pass through the window will be significant, which will significantly alter the LO measurement with and without the chopper (for thin windows as used here, this effect can mostly be neglected). A downside of the heterodyne technique is that it is experimentally demanding, requiring micrometer accuracy in the path length of the beams between sample and reference surfaces to ensure long-term phase stability. In contrast, our technique requires only mm to cm stability in the distance between sample and reference surfaces distance (depending on the probe wavelength), which is trivially achieved. The other significant advantage of the technique we present here is the short times required to achieve good S/N in time-resolved measurements. In the present case, this was of the order of 10 s to minutes compared to ~50 min/delay for a heterodyne measurement.[32] This advantage is a trade-off achieved mainly by not recording the full spectral information, although we note that, to gain useful spectral information for electronic transitions would require a substantial bandwidth (>100 nm).

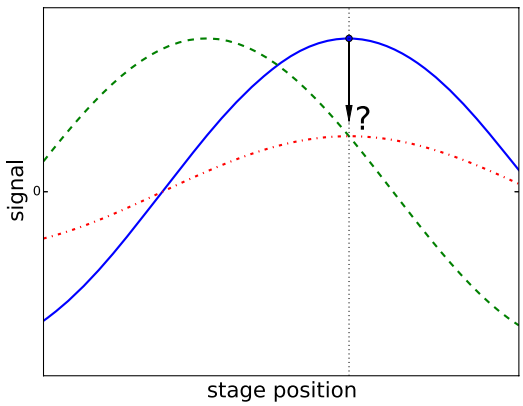

FIG. 6. An illustration of the ambiguity inherent in taking a measurement at a single stage position (marked as the vertical black dotted line). It is unclear if the change in signal of a measurement (blue solid line) is due to a change in intensity (red dots and dashes) or a change in phase (green dashes).

V. CONCLUSIONS

A time-resolved technique for studying the dynamics of adsorbates residing at the interface between two centrosymmetric media has been developed. The method is in essence an improvement to phase-sensitive SHG measurements that use interference between the SHG electric field from the sample and a local oscillator SHG field (LO) from a reference. By means of a lock-in measurement between an interfering SHG and LO pair and a non-interfering pair, the large constant offset can be removed leaving only the interference terms. The final signal is shown to be phase-sensitive and linear with concentration. The absolute phase has been calibrated to that of quartz enabling the measurement of the real and imaginary parts of the second order hyperpolarizability. The linearity of the signal means that the signal is more sensitive at low concentrations compared to conventional time-resolved SHG spectroscopy. The applicability is demonstrated on the dynamics of malachite green at the water/air interface, for which we show that excellent time-resolved dynamics can be obtained in short acquisition times. We compare our methodology to similar methods, in particular the popular heterodyne detected SFG method.

ACKNOWLEDGMENTS

We are grateful to Laurence Stanley for constructing the motorized delay state and to the Leverhulme Trust and the ERC (Starting Grant No. 306536) for funding.

[1]R. W. Boyd, *Nonlinear Optics*, 3rd ed. (Elsevier Science, 2008).
[2]Y. R. Shen, *The Principles of Nonlinear Optics* (Wiley-Interscience, 2003).

This article is copyrighted as indicated in the article. Reuse of AIP content is subject to the terms at: http://scitation.aip.org/termsconditions. Downloaded to IP: 129.234.252.66 On: Thu, 26 Mar 2015 14:17:19

[3]Y. R. Shen, Nature **337**(6207), 519-525 (1989).
[4]K. B. Eisenthal, Chem. Rev. **96**(4), 1343-1360 (1996).
[5]G. L. Richmond, Chem. Rev. **102**(8), 2693-2724 (2002).
[6]F. M. Geiger, Annu. Rev. Phys. Chem. **60**(1), 61-83 (2009).
[7]A. M. Jubb, W. Hua, and H. C. Allen, Annu. Rev. Phys. Chem. **63**(1), 107-130 (2012).
[8]D. M. Sagar, C. D. Bain, and J. R. R. Verlet, J. Am. Chem. Soc. **132**(20), 6917-6919 (2010).
[9]R. K. Chang, J. Ducuing, and N. Bloembergen, Phys. Rev. Lett. **15**(1), 6-8 (1965).
[10]Y. R. Shen, Annu. Rev. Phys. Chem. **64**(1), 129-150 (2013).
[11]G. Berkovic, Y. R. Shen, G. Marowsky, and R. Steinhoff, J. Opt. Soc. Am. B **6**(2), 205-208 (1989).
[12]T. Rasing, Y. R. Shen, M. W. Kim, and S. Grubb, Phys. Rev. Lett. **55**(26), 2903-2906 (1985).
[13]H. W. K. Tom, T. F. Heinz, and Y. R. Shen, Phys. Rev. Lett. **51**(21), 1983-1986 (1983).
[14]R. Superfine, J. Y. Huang, and Y. R. Shen, Opt. Lett. **15**(22), 1276-1278 (1990).
[15]Q. Du, E. Freysz, and Y. R. Shen, Phys. Rev. Lett. **72**(2), 238-241 (1994).
[16]V. Ostroverkhov, G. A. Waychunas, and Y. R. Shen, Phys. Rev. Lett. **94**(4), 046102 (2005).
[17]N. Ji, V. Ostroverkhov, C. Y. Chen, and Y. R. Shen, J. Am. Chem. Soc. **129**(33), 10056-10057 (2007).
[18]N. Ji, V. Ostroverkhov, C. S. Tian, and Y. R. Shen, Phys. Rev. Lett. **100**(9), 096102 (2008).
[19]K. J. Veenstra, A. V. Petukhov, A. P. de Boer, and T. Rasing, Phys. Rev. B **58**(24), 16020-16023 (1998).
[20]P. T. Wilson, Y. Jiang, O. A. Aktsipetrov, E. D. Mishina, and M. C. Downer, Opt. Lett. **24**(7), 496-498 (1999).
[21]S. Yamaguchi and T. Tahara, J. Chem. Phys. **129**(10), 101102 (2008).
[22]I. V. Stiopkin, H. D. Jayathilake, A. N. Bordenyuk, and A. V. Benderskii, J. Am. Chem. Soc. **130**(7), 2271-2275 (2008).
[23]S. Nihonyanagi, S. Yamaguchi, and T. Tahara, J. Chem. Phys. **130**(20), 204704 (2009).
[24]H. Watanabe, S. Yamaguchi, S. Sen, A. Morita, and T. Tahara, J. Chem. Phys. **132**(14), 144701 (2010).
[25]J. A. Mondal, S. Nihonyanagi, S. Yamaguchi, and T. Tahara, J. Am. Chem. Soc. **132**(31), 10656-10657 (2010).
[26]W. Hua, X. K. Chen, and H. C. Allen, J. Phys. Chem. A **115**(23), 6233-6238 (2011).
[27]A. Kundu, S. Yarnaguchi, and T. Tahara, J. Phys. Chem. Lett. **5**(4), 762-766 (2014).
[28]R. E. Pool, J. Versluis, E. H. G. Backus, and M. Bonn, J. Phys. Chem. B **115**(51), 15362-15369 (2011).
[29]W. Xiong, J. E. Laaser, R. D. Mehlenbacher, and M. T. Zanni, Proc. Natl. Acad. Sci. **108**(52), 20902-20907 (2011).
[30]S. Nihonyanagi, J. A. Mondal, S. Yamaguchi, and T. Tahara, Annu. Rev. Phys. Chem. **64**(1), 579-603 (2013).
[31]K. Watanabe, K. Inoue, I. F. Nakai, and Y. Matsumoto, Phys. Rev. B **81**(24), 241408 (2010).
[32]S. Nihonyanagi, P. C. Singh, S. Yamaguchi, and T. Tahara, Bull. Chem. Soc. Jpn. **85**(7), 758-760 (2012).
[33]R. Stolle, G. Marowsky, E. Schwarzberg, and G. Berkovic, Appl. Phys. B: Lasers Opt. **63**(5), 491-498 (1996).
[34]See supplementary material at http://dx.doi.org/10.1063/1.4909522 for a consideration of the offset in the signal and the details of the calculation of the theoretical curves in Figure 3.
[35]J. G. Brainerd, A. G. Jensen, and L. G. Cumming, Proc. IRE **37**(12), 1378-1395 (1949).
[36]R. C. Miller and W. A. Nordland, Phys. Rev. B **2**(12), 4896-4902 (1970).
[37]N. Bloembergen and P. S. Pershan, Phys. Rev. **128**(2), 606-622 (1962).
[38]X. Shi, E. Borguet, A. N. Tarnovsky, and K. B. Eisenthal, Chem. Phys. **205**(1-2), 167-178 (1996).
[39]P. Sen, S. Yamaguchi, and T. Tahara, Faraday Discuss. **145**, 411-428 (2010).
[40]K. Kemnitz, K. Bhattacharyya, J. M. Hicks, G. R. Pinto, K. B. Eisenthal, and T. F. Heinz, Chem. Phys. Lett. **131**(4-5), 285-290 (1986).

This article is copyrighted as indicated in the article. Reuse of AIP content is subject to the terms at: http://scitation.aip.org/termsconditions. Downloaded to IP: 129.234.252.66 On: Thu, 26 Mar 2015 14:17:19